Formation and Magnetic Properties of Hemin-Azide-$(CH_3)_2SO$, a Model Complex for Azide Catalase[1]

Saburo Neya and Isao Morishima*

Contribution from the Department of Hydrocarbon Chemistry, Faculty of Engineering, Kyoto University, Kyoto 606, Japan. *Received November 9, 1981*

Abstract: Binding of azide to ferric protohemin in dimethyl sulfoxide was examined by a visible absorption method, and a new type of 6-coordinate compound, hemin-N_3^--$(CH_3)_2SO$, was found, with a formation constant of 3.02×10^3 M^{-1}. The visible, infrared, and electron spin resonance spectra of this compound suggested the presence of a thermal spin equilibrium between the high- and low-spin states. The thermodynamics parameters of the equilibrium were determined to be $\Delta H = -136$ cal/mol and $\Delta S = -0.975$ eu by the magnetic susceptibility measurement with a Faraday balance. The coordination structure of this complex is similar to that of the prosthetic group of azide catalase with proximal tyrosine. Comparison of the thermodynamic values between azide catalase and the model suggests a sizable contribution from the nonbonded interactions around the heme to the ΔH and ΔS values of azide catalase. This result shows that spin equilibrium is primarily induced by the axial ligands and that the equilibrium is further modulated by the nonbonded interactions in the heme pocket.

The magnetic properties of hemoprotein have been extensively studied for various ligand complexes.[2-7] Among the derivatives examined, the azide complex with an intermediate ligand field strength has been reported to exhibit a temperature-dependent spin equilibrium between the high- and low-spin states.[4-7] The analysis of the equilibrium in azide hemoprotein provided structural information relevant to the function. Available evidence suggested the importance of the porphyrin-globin interaction to modulate spin equilibrium.[2-8] The protein influence may be evaluated by considering the spin equilibrium of a simple porphyrin complex. From this research interest, several model complexes for azide hemoprotein have been reported. Huang and Kassner[9] analyzed the spin equilibrium of the azide complex of a heme peptide obtained from cytochrome *c*. Adams et al.[10] determined the molecular structure of iron(III) tetraphenylporphyrin-azide-pyridine and identified its low-spin state. Neya and Morishima[11] analyzed the paramagnetic NMR shifts of hemin-N_3^--(1-methyl- or 2-methylimidazole) and suggested that distortion of the Fe(III)-N(imidazole) bond could modulate the spin equilibrium of the model complex.

We report here the formation of a new type of azide complex, hemin-N_3^--$(CH_3)_2SO$. Experiments are described which show that this compound exhibits thermal spin equilibrium. Control experiments were performed for a corresponding 5-coordinate high-spin complex, hemin-N_3^-. The effect of the coordination number on the thermal spin equilibrium was examined, and the visible absorption, EPR, and IR spectra and the magnetic susceptibility of hemin-N_3-$(CH_3)_2SO$ were characterized. The relevance of the results to hemoprotein, especially to catalase with proximal tyrosine,[12] is now discussed.

Materials and Methods

Chemicals. Protohemin chloride (type I) was obtained from Sigma, and NaN_3, $CHCl_3$, and $(CH_3)_2SO$ were obtained from Nakarai Chemicals Ltd., Kyoto, Japan. Azide hemin dimethyl ester was prepared by the method of McCoy and Caughey.[13] The 6-coordinate hemin-N_3^--$(CH_3)_2SO$ was prepared by dissolving hemin chloride into $(CH_3)_2SO$ containing sufficient NaN_3 to saturate the heme iron.

EPR Spectra. The X-band EPR spectra were recorded on a JEOL JES-FE-3X spectrometer at 77 K operating in a 100-kHz magnetic field modulation. Temperature-dependent EPR spectra in a 77-163 K range were also recorded at JEOL, Tokyo. The *g* values were determined by using Mn(II) ($g = 1.981$) in MgO as a field marker.

IR Spectra. The IR spectra of azide hemins in $CHCl_3$ or $(CH_3)_2SO$ were recorded in a 1900-2200-cm^{-1} range at 21 °C with a JASCO A-302 spectrometer. KBr IR cells with a 0.1-mm path length were used.

Visible Absorption Spectra. Visible absorption spectra at room temperature were recorded with a Union-Giken SM-401 spectrometer by using quartz cells with 1-cm path length. The spectra at low temperature were recorded with a Union-Giken SM-401 spectrometer at Keio University by using a special attachment designed by Hagihara and Iizuka,[14] as described by Makino et al.[15]

Magnetic Susceptibility Measurement. Magnetic susceptibility of hemin in $(CH_3)_2SO$ containing 0.8 M NaN_3 was measured with a Shimadzu Faraday balance, Type MB-2. $CrK(SO_4)_2 \cdot 12H_2O$ was used as a primary standard with a paramagnetic susceptibility of 0.622×10^{-2} cgs emu at 300 K.[16] Diamagnetic susceptibility of hemin-N_3^--$(CH_3)_2SO$ was calculated from Pascal's constants[17] and from the value reported for protophorphyrin dimethyl ester.[18]

Results

Formation of Hemin-N_3^--$(CH_3)_2SO$. Figure 1 shows the Soret absorption changes on azide binding to hemin in $(CH_3)_2SO$. Addition of NaN_3 resulted in a sizable decrease in the peak intensity, with isosbestic points at 385 and 415 nm. The change was analyzed according to the equlibrium scheme:

$$P + N_3^- \overset{K}{\rightleftharpoons} P \cdot N_3^-$$

where P is protohemin (axial ligands are not shown) and K is a constant defined as $K = [P \cdot N_3^-]/[P][N_3^-]$. The absorption change at 405 nm was analyzed by the Hill equation:

$$\log (Y/(1 - Y)) = n \log [N_3^-] + C$$

(1) This work was supported by a Grant-in-Aid for Scientific Research from the Ministry of Education, Science and Culture, Japan.

(2) Iizuka, T.; Yonetani, T. *Adv. Biophys.* **1970**, *1*, 157-182.
(3) Iizuka, T.; Kotani, M.; Yonetani, T. *Biochim. Biophys. Acta* **1968**, *167*, 257-267.
(4) Beetlestone, J.; George, P. *Biochemistry* **1964**, *3*, 707-714.
(5) Iizuka, T.; Kotani, M.; Yonetani, T. *J. Biol. Chem.* **1971**, *246*, 4731-4736.
(6) (a) Iizuka, T.; Kotani, M. *Biochim. Biophys. Acta* **1969**, *194*, 351-363. (b) Morishima, I.; Iizuka, T. *J. Am. Chem. Soc.* **1974**, *96*, 5279-5283. (c) Iizuka, T.; Morishima, I. *Biochim. Biophys. Acta* **1974**, *371*, 1-13. (d) Morishima, I.; Neya, S.; Inubushi, T.; Yonezawa, T.; Iizuka, T. *Ibid.* **1978**, *534*, 307-316.
(7) Messana, C.; Cerdonio, M.; Shenkin, P.; Noble, R. W.; Fermi, G.; Perutz, R. N.; Perutz, M. F. *Biochemistry* **1978**, *17*, 3652-3662.
(8) Ohtsuka, J. *Biochim. Biophys. Acta* **1970**, *214*, 233-235.
(9) Huang, Y.-P.; Kassner, R. J. *J. Am. Chem. Soc.* **1979**, *101*, 5807-5810.
(10) Adams, K.; Rasmussen, P. G.; Scheidt, R. W.; Hatano, K. *Inorg. Chem.* **1979**, *18*, 1892-1899.
(11) Neya, S.; Morishima, I. *Biochemistry* **1980**, *19*, 258-265.
(12) Murthy, M. R. N. Reid, T. J., III; Siciganano, A.; Tanaka, N.; Rossman, M. G. *J. Mol. Biol.* **1981**, *152*, 465-499.
(13) McCoy, S.; Caughey, W. S. *Biochemistry* **1970**, *9*, 2387-2393.
(14) Hagihara, B.; Iizuka, T. *J. Biochem. (Tokyo)* **1971**, *69*, 355-362.
(15) Makino, R.; Sakaguchi, K.; Iizuka, T.; Ishimura, Y. *J. Biol. Chem.* **1981**, *255*, 11883-11891.
(16) König, E. "Landolt-Börnstein Numerical Data and Functional Relationships in Science and Technology, New Series, Group II"; Hellewege, K.-H., Hellewege, M. M., Eds.; Springer-Verlag: New York, 1966; Vol. 2.
(17) Boudreaux, E. A.; Mulay, L. N. "Theory and Applications of Molecular Paramagneticism"; Wiley: New York, 1976; pp 491.
(18) Eaton, S. S.; Eaton, G. R. *Inorg. Chem.* **1980**, *19*, 1096-1098.

0002-7863/82/1504-5658$01.25/0

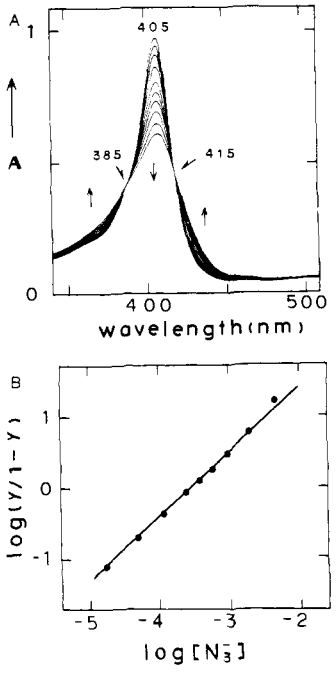

Figure 1. Spectroscopic titration of protohemin with NaN_3 in $(CH_3)_2SO$ at 21 °C. (A) Soret absorption changes. Azide concentration increases as indicated by the arrows. (B) Hill plots of azide binding equilibrium of hemin with $n = 0.97 \pm 0.01$ and $K = (3.02 \pm 0.12) \times 10^3$ M^{-1}. Monitored at 405 nm.

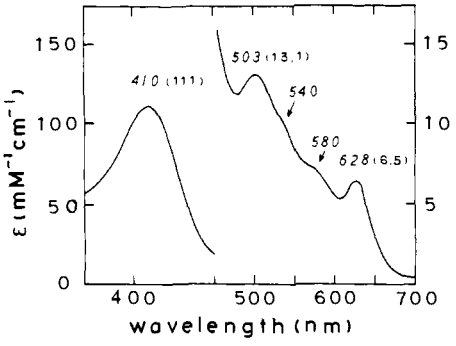

Figure 2. Visible absorption spectrum of hemin-N_3^--$(CH_3)_2SO$ in $(CH_3)_2SO$ containing 0.1 M NaN_3 at 21 °C.

where Y and n are the fractional formation of the complex and the slope of the Hill plots, respectively, and C is a constant. The plot of log $(Y/(1-Y))$ vs. log $[N_3^-]$ (Figure 1B) yielded a straight line with $n = 1$, consistent with a 1:1 complex formation. The azide binding constant K was $(3.02 \pm 0.12) \times 10^3$ M^{-1}, and the extinction coefficient of the Soret peak of the complex was determined to be 111 ± 2 mM^{-1} cm^{-1} on the basis of $\epsilon = 174$ mM^{-1} cm^{-1} for the Soret peak or protohemin in $(CH_3)_2SO$.[19]

It should be noted that 2 mol of $(CH_3)_2SO$ bind to iron(III)·porphyrin to form the bis coordinate complex.[20,21] Hence, the present monoazide complex formed in $(CH_3)_2SO$ is to be characterized as hemin-N_3^--$(CH_3)_2SO$. Figure 2 shows the visible absorption spectrum of this complex. The Soret peak is much depressed, and the charge-transfer bands at 500 and 630 nm are dominant, though the 540- and 580-nm bands are still observable.

EPR Spectra. Figure 3 compares the EPR spectrum of protohemin in $(CH_3)_2SO$ containing a saturating amount of NaN_3 with that of hemin-N_3^- in $CHCl_3$. In Figure 3B, the high-spin peak around $g = 6$ and low-spin peaks with $g = 2.81$, 2.16, and 1.75 were concomitantly observed, while only the high-spin signal

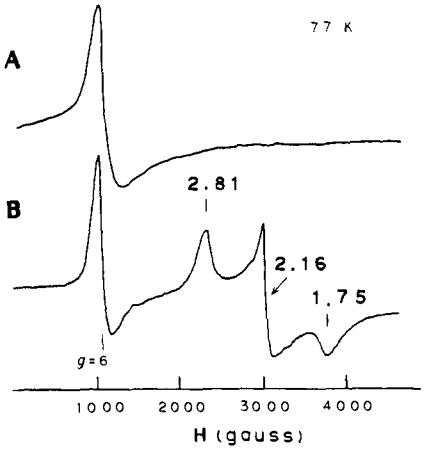

Figure 3. EPR spectra of the azide complexes at 77 K. (A) Hemin-N_3^- dimethyl ester in $CHCl_3$; (B) hemin-N_3^--$(CH_3)_2SO$ in $(CH_3)_2SO$ containing 0.8 M NaN_3.

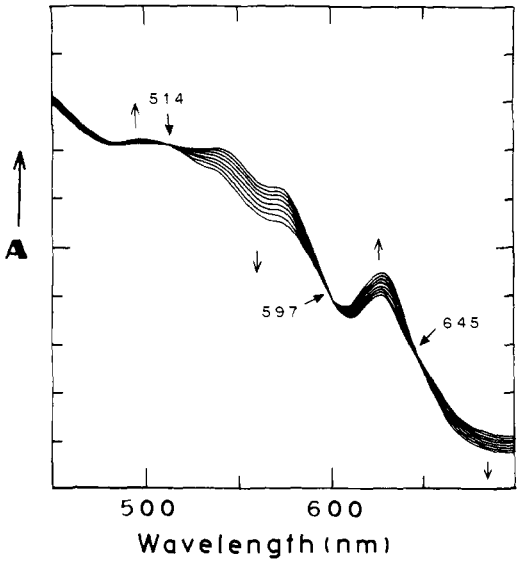

Figure 4. Visible absorption spectra of hemin-N_3^--$(CH_3)_2SO$ in the 84–194 K range. Temperature rises as indicated by the arrows. In $(CH_3)_2SO$ containing 0.1 M NaN_3 and 50 μM protohemin.

is shown in Figure 3A. The high- and low-spin peaks in Figure 3B seem to arise not from a mixture of two purely high- and low-spin components with different coordination structures but from a single species, hemin-N_3^--$(CH_3)_2SO$, in view of the azide binding result in Figure 1. The low-spin g values in Figure 3B ($g = 2.81$, 2.16, and 1.75) are closely similar to those of the azide complexes of myoglobin ($g = 2.80$, 2.22, and 1.72),[22] catalase ($g = 2.80$, 2.18 and 1.74),[23] and cytochrome c ($g = 2.73$, 2.30, and 1.81).[24] The present result shows that hemin-N_3^--$(CH_3)_2SO$ is in a spin equilibrium similar to that in various azide hemoproteins.[2,5,7,22,23,25]

The temperature dependence of the EPR spectrum of hemin-N_3—$(CH_3)_2SO$ was examined in a 77–163 K range. The EPR spectrum was more low-spin type at 77 than at 163 K. The line width of the EPR peaks was considerably broadened with increasing temperature to make quantitative analysis of the high- and low-spin components difficult. Thus, the variable-temperature EPR measurements were unsuccessful for the quantitative analysis of thermal spin equilibrium. This is also the case for the spin-

(19) Brown, S. R.; Lantzke, I. S. *Biochem. J.* **1969**, *115*, 279–285.
(20) Zobrist, M.; La Mar, G. N. *J. Am. Chem. Soc.* **1978**, *100*, 1944–1946.
(21) Mashiko, T.; Kastner, M. E.; Spartalian, K.; Scheidt, W. R.; Reed, C. A. *J. Am. Chem. Soc.* **1978**, *100*, 6354–6362.
(22) Hori, H. *Biochim. Biophys. Acta* **1971**, *251*, 227–235.
(23) Torii, K.; Iizuka, T.; Ogura, Y. *J. Biochem. (Tokyo)* **1971**, *68*, 837–841.
(24) Ikeda-Saito, M.; Iizuka, T. *Biochim. Biophys. Acta* **1975**, *393*, 335–342.
(25) Brill, A. S.; Williams, R. J. P. *Biochem. J.* **1961**, *78*, 246–253.

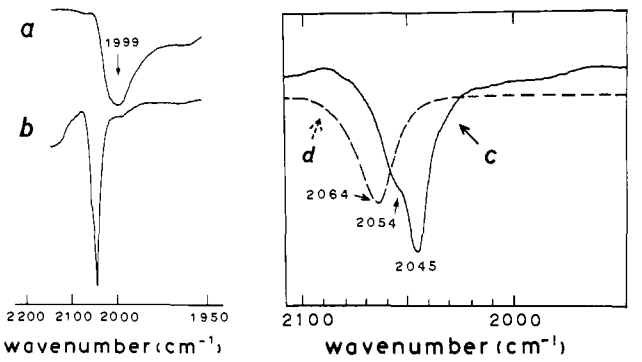

Figure 5. Infrared azide stretching band at 21 °C. (a) Free azide ion in $(CH_3)_2SO$; (b) hemin-N_3^--$(CH_3)_2SO$ in $(CH_3)_2SO$; (c) hemin-N_3^--$(CH_3)_2SO$ in $(CH_3)_2SO$ (expanded); (d) hemin dimethyl ester-N_3^- in $CHCl_3$.

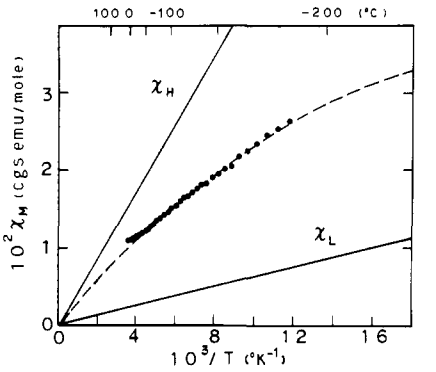

Figure 6. Temperature dependence of the paramagnetic susceptibility of hemin-N_3^--$(CH_3)_2SO$ in $(CH_3)_2SO$ at [hemin] = 48 mM and [NaN_3] = 0.8 M. The dashed curve is the least-squares fit calculated with $\Delta H = -136$ cal/mol and $\Delta S = -0.975$ eu. The lines with χ_H and χ_L correspond to the purely high- and low-spin values, respectively.

equilibrium analysis of cytochrome *c* peroxidase by EPR.[2]

Visible Absorption Spectra at Low Temperatures. Brill and Williams[25] reported that visible absorption intensity is diagnostic of the spin state of heme iron. Iizuka and Kotani[5] reported a close relationship between optical and magnetic properties of various hemoprotein complexes. For the qualitative analysis of the spin equlibrium in hemin-N_3^--$(CH_3)_2SO$, the temperature-dependent visible absorption spectra were recorded. Figure 4 shows that the low-spin bands around 540 and 570 nm are more dominant at 86 K than at 21 °C (Figure 2). The intensity of the low-spin bands increased with decreasing temperature, with isosbestic points at 514, 597, and 645 nm corresponding to a color change of the sample from greenish- to reddish-brown at the lower temperature. The changes were fully reversible. It should be noted that the visible absorption spectrum of the frozen sample, in which ligand exchange does not occur, changes with temperature. This is in agreement with the interpretation of the above EPR result that suggests that the high- and low-spin EPR peaks arise from a single species.

An increase in the low-spin visible absorption bands at lower temperatures suggests a low-spin ground state in hemin-N_3^--$(CH_3)_2SO$. In contrast, the visible absorption of 5-coordinate hemin-N_3^- in $CHCl_3$ did not show temperature-dependent change.

IR Spectra. The IR spectra have provided an effective probe of azide binding to hemoproteins.[13,26] Figure 5 shows the IR spectra of free and iron-bound azide molecules in $(CH_3)_2SO$. To minimize the amount of free azide ion, we prepared the azide complex by adding sufficient azide to saturate the heme iron incompletely. The expanded spectrum in Figure 5 shows that the 2054-cm^{-1} peak overlaps the 2045-cm^{-1} peak with a comparable intensity in the hemin-N_3^--$(CH_3)_2SO$ spectrum, while hemin-N_3^- exhibits a single IR band at 2064 cm^{-1}. The existence of the two IR bands indicates that the iron-bound azide in hemin-N_3^--$(CH_3)_2SO$ can assume two different binding mode, i.e., the high- and low-spin states. This is consistent with the EPR (Figure 3) and low-temperature visible absorption (Figure 4) results. The 2054-cm^{-1} band was assigned to the high-spin form and the 2045-cm^{-1} band to the low spin form from the IR spectral analogy of the azide complexes of hemoglobin (2046 cm^{-1}, high spin; 2025 cm^{-1}, low spin) and myoglobin (2043 cm^{-1}, high spin; 2023 cm^{-1}, low spin).[13,26]

Paramagnetic Susceptibility. For the quantitative and direct determination of the thermodynamic parameters of spin equilibrium, the magnetic susceptibility of hemin-N_3^--$(CH_3)_2SO$ was measured in frozen $(CH_3)_2SO$ with a Faraday balance. The temperature dependence of the paramagnetic susceptibility is shown in Figure 6. The results were analyzed by assuming an equilibrium between the two states

$$\text{high spin} \overset{K}{\rightleftharpoons} \text{low spin}$$

where K = [low spin]/[high spin] = $\alpha/(1-\alpha)$. The presence of such an equilibrium is very likely from the EPR, visible absorption, and IR results presented above. The observed paramagnetic susceptibility χ is expressed as

$$\chi = \chi_L\alpha + \chi_H(1-\alpha)$$

where χ_L and χ_H are the paramagnetic susceptibilities of the pure low- and high-spin states.[23,27] Plots of log K vs. $1/T$ gave a straight line with $\Delta H = -136 \pm 2$ cal/mol and $\Delta S = -0.975 \pm 0.012$ eu. The temperature dependence of the χ value in Figure 6 is similar to that of azide catalase as reported by Torii et al.[23,27] The dashed curve in Figure 6 is the least-squares fit calculated with these ΔH and ΔS. The compensation temperature T_c, where the high- and low-spin states are equally populated, was determined to be 139.5 ± 3.8 K. The calculated low-spin fractions were $\alpha = 0.43$ (4.72 μ_B) at 300 K and $\alpha = 0.60$ (4.14 μ_B) at 77 K, consistent with the visible absorption, EPR, and IR evidences in Figures 3, 4, and 5.

Discussion

The thermal equilibrium between the high- and low-spin states has been reported to be a unique property of hemoprotein. However, Huang and Kassner[9] demonstrated that spin equilibrium is observed in the azide complex of the heme peptide obtained from cytochrome *c*, suggesting that spin equilibrium is not characteristic of hemoprotein. Hill and Morallee[28] also reported a thermal spin equilibrium in another kind of porhyrin complex, iron(III) octaethylporphyrin bis(3-chloropyridine). The present spectroscopic and magnetic susceptibility results suggest that the 6-coordinate complex, hemin-N_3^--$(CH_3)_2SO$, is in a spin equilibrium. This is the simplest azide hemin system that exhibits spin equilibrium.

It should be noted that hemin-N_3^- and hemin-$2(CH_3)_2SO$ are high spin, while hemin-N_3^--$(CH_3)_2SO$ is in a spin equilibrium. The appearance of the low-spin state in this mixed-ligand complex suggests that spin equilibrium is primarily determined by the ligand trans to the azide. Adams et al.[10] reported that iron(III) tetraphenylporphyrin-N_3^--pyridine is low spin, and Neya and Morishima[11] reported that substitution with 2-methylimidazole in hemin-N_3^--(1-methylimidazole) could induce a shift toward the high-spin side of the equilibrium. These trans-ligand effects may be associated with a change in the Fe(III)-ligand bond length. Indeed, X-ray analyses of tris(*N*,*N*-diethyldithiocarbamate)-iron(III) at two temperatures showed that a 0.05-Å decrease in the Fe(III)-ligand distance caused an ~45% shift of the equilibrium to the low-spin side (4.3 and 2.2 μ_B at 297 and 79 K, respectively.)[29] Recent X-ray results of iron(III) octaethylporphyrin bis(3-chloropyridine) show that the Fe(III)-N(3-chloropyridine) distance is 2.043 and 2.316 Å at 98 and 293 K, respectively, and that the longer Fe(III)-ligand distance is as-

(26) Alben, J. O.; Fager, L. Y. *Biochemistry* **1972**, *11*, 842-847.

(27) Torii, K. *Kagaku no Ryoiki* **1969**, *23*, 812-822.
(28) Hill, H. A. O.; Morallee, K. G. *J. Am. Chem. Soc.* **1972**, *94*, 731-738.
(29) Leipoldt, J. G.; Coppens, P. *Inorg. Chem.* **1973**, *12*, 2269-2274.

Table I. Thermodynamic Values for the Spin Equilibrium of the Azide Complexes

	ΔH, cal/mol	ΔS, eu	T_c,[a] K	K_{25}[b]	low-spin fraction at 25 °C	ref
hemoglobin	-5094	-13.62	374	5.8	0.85	6
	-6700	-17	400	16	0.94	13
myoglobin	-3746	-9.58	391	4.5	0.81	6
	-2740	-6.8	403	3.3	0.77	4
heme peptide	-3890	-8.6	452	9.4	0.90	9
catalase	-505	-5.8	87	0.13	0.11	27
hemin-N_3^--$(CH_3)_2SO$	-136	-0.975	139.5	0.77	0.43	this work

[a] Compensation temperature, where the high- and low-spin states are equally populated. [b] Equilibrium constant = [low spin]/[high spin] at 25 °C.

sociated with the higher spin state (2.9 and 4.7 μ_B at 100 and 294 K, respectively).[30] Thus the decreased low-spin character of hemin-N_3^--$(CH_3)_2SO$ may be related to an increased Fe(III)-$OS(CH_3)_2$ bond length due to an increased thermal motion of the ligated $(CH_3)_2SO$ at higher temperatures. In the extreme of complete rupture of the Fe(III)-$OS(CH_3)_2$ bond, the azide complex is high spin, as evidenced in the EPR and IR spectra of 5-coordinate hemin-N_3^- in Figures 3 and 5.

Although $(CH_3)_2SO$ is not a physiologically meaningful ligand, ligation of an oxygenous base to heme iron may have a relevance to the prosthetic structure of azide catalase.[23,27] Recent X-ray analysis on beef liver catalase demonstrated tyrosine-357 as the proximal heme ligand.[12] Table I compares the thermodynamic values associated with the spin equilibrium in several azide complexes with those of the nitrogen or oxygen axial base. The ΔH and ΔS of catalase and hemin-N_3^--$(CH_3)_2SO$ are similar to each other and much smaller than those of hemoglobin and myoglobin. The similarity of ΔH, ΔS, and EPR g values (Figure 3) between catalase and the hemin-N_3^--$(CH_3)_2SO$ is consistent with the oxygenous base being the proximal ligand in catalase.[12] However, ΔS of the model is about 5-fold less negative than that of catalase. This is expected from the lack of the rearrangement of the nonbonded interactions in hemin-N_3^--$(CH_3)_2SO$ between porphyrin and globin with temperature change. Comparison of ΔH and K_{25} values in Table I suggests that the stabilization of the low-spin state tends to be associated with a more negative ΔH. Significantly negative ΔH's in the imidazole-ligated complexes may be explained in terms of a stronger axial ligation of histidine than of tyrosine, suggesting an enthalpy effect on spin equilibrium derived from the axial ligand difference.

The appearance of the spin equilibrium in the present model complex suggests that the spin equilibrium in azide catalase is primarily determined by the axial ligands and that the equilibrium is further modulated by the stereochemical changes of the globin surrounding the heme. A comparison of ΔH and ΔS between catalase and hemin-N_3^--$(CH_3)_2SO$ suggests a sizable contribution from the nonbonded interaction to the thermodynamic values in catalase. It is therefore likely that the nonbonded interaction could change the geometry of the Fe(III)-O(Tyr-357) bond[12] and the Fe(III) displacement to modulate the spin equilibrium in azide catalase.

Acknowledgment. We are grateful to Dr. H. Kobayashi (magnetic susceptibility measurement), Drs. Y. Sugiura, M. Chikira, and M. Kohno (EPR measurements), Drs. S. Nishimoto and H. Yamada (IR measurement), and Drs. R. Makino, T. Iizuka, and Y. Ishimura (visible spectra at low temperature) for their generous collaborations. Helpful discussions with these authors during the measurements are gratefully appreciated. Continuous encouragement of Dr. T. Yonezawa is also acknowledged.

Registry No. Hemin-N_3-$(CH_3)_2SO$, 82917-91-7; catalase, 9001-05-2.

(30) Scheidt, W. R.; Geiger, D. K.; Haller, K. J. *J. Am. Chem. Soc.* **1982**, *104*, 495-499.

Complexation of Calcium by the Synthetic Ionophore McN-4308, [2-(4-(Diphenylmethyl)-1-piperidinyl)-2-oxoethoxy]acetic Acid. Crystal and Molecular Structure of the Free Acid and of the Calcium Complex

Patrick Van Roey,*[1] G. David Smith,[1] William L. Duax,[1] Michael J. Umen,[2] and Bruce E. Maryanoff[2]

Contribution from the Medical Foundation of Buffalo, Inc., Buffalo, New York 14203, and McNeil Pharmaceutical, Spring House, Pennsylvania 19477. *Received March 3, 1982*

Abstract: McN-4308 is a synthetic monocarboxylic acid that exhibits the properties of a calcium ionophore. We have studied the crystal structures of McN-4308 and its calcium complex. The free acid crystallizes in space group $P2_1/c$ with cell dimensions a = 20.244 (4) Å, b = 5.822 (2) Å, c = 16.363 (4) Å, β = 95.85 (2)°, and Z = 4. The diglycolamic acid moiety shows conformational flexibility about the O3-C3 and the C1-C2 bonds. The calcium complex of McN-4308 crystallizes in space group $P\bar{1}$, a = 17.460 (1) Å, b = 18.089 (1) Å, c = 15.834 (1) Å, α = 97.24 (1)°, β = 88.24 (1)°, γ = 113.74 (1)° with four calcium ions, each coordinated by two ionophores, in the unit cell (Z = 4). The complex exists in the solid state as centrosymmetric dimers possessing two calcium cations, four ionophore anions, and two water molecules. The calcium ions are eight-coordinate with square antiprism geometry. The two dimers observed in the unit cell are stereoisomers but have very similar overall geometry. In contrast to the free acid, the ionophores in the complex have nearly planar diglycolamic moieties. The dimers are held together through bridging carboxylate groups of two of the ionophores.

Ionophores are compounds that facilitate the transport of ions across natural and artificial membranes. They have been studied primarily as potential drugs and as tools to help understand ion transport in biological systems. Until recently, most known

0002-7863/82/1504-5661$01.25/0